Journal of Advances in Medical and Biomedical Research | ISSN:2676-6264

# Green Synthesis and Characterization of Silver Nanoparticles Using *Heracleum persicum* Fruit Extract and Their Cytotoxicity on MCF-7 Cells

**Ali Sharafi [1,2], Somayeh Sadighian [2], Banafsheh Raeisi [2] Zahra Gharari [2], Alireza Yazdinezhad [2*]**

1. *Zanjan Pharmaceutical Biotechnology Research Center, Zanjan University of Medical Sciences, Zanjan, Iran*
2. *Department of Pharmacognosy and Pharmaceutical Biotechnology, School of Pharmacy, Zanjan University of Medical Sciences, Zanjan, Iran*

**Article Info**

**Received**: 2026/06/09;

**Accepted**: 2026/07/01;

**Published Online:** 2026/10/18;

***Corresponding author:**

**Alireza Yazdinezhad,**

Department of Pharmacognosy and Pharmaceutical Biotechnology, School of Pharmacy, Zanjan University of Medical Sciences, Zanjan, Iran

**Email:** yazd1387@gmail.com

**How to Cite This Article:**

Sharafi A, Sadighian S, Raeisi B, Gharari Z, Yazdinezhad A. Green Synthesis and Characterization of Silver Nanoparticles Using *Heracleum persicum* Fruit Extract and Their Cytotoxicity on MCF-7 Cells. J Adv Med Biomed Res 2026; 34(5):420-429.

**ABSTRACT**

**Background & Objective:** *Heracleum persicum* (Persian hogweed) is traditionally utilized as a spice in Iran and is rich in diverse phytochemicals, including flavonoids, alkaloids, furanocoumarins, and volatile oils. This study aimed to exploit these metabolites for the biosynthesis of silver nanostructures (AgNPs) and to evaluate their cytotoxicity against malignant human MCF-7 breast cancer cells. This approach highlights the novelty of using *H. persicum* fruit extract as a natural reducing and capping agent, which has not been previously reported for biomedical nanoparticle applications.

**Materials & Methods:** AgNPs were synthesized using an aqueous fruit extract, with reaction parameters optimized to maximize yield. The physicochemical properties of the synthesized nanostructures, including morphology, size distribution, crystallinity, and stability, were characterized via UV–Vis spectroscopy, transmission electron microscopy (TEM), X-ray diffraction (XRD), dynamic light scattering (DLS), and zeta potential analysis. The anti-proliferative potential against MCF-7 cells was quantified using the MTT assay.

**Results:** Optimization revealed that a 1:1 ratio of fruit extract to 3 mM silver nitrate (AgNO3) yielded the most efficient synthesis. Characterization confirmed the formation of spherical nanoparticles with a size distribution ranging from 60 to 600 nm. Biological evaluation using the MTT assay demonstrated potent inhibition of MCF-7 cell proliferation, with $IC_{50}$ values of 10.42 µg/mL at 24 h and 8.92 µg/mL at 48 h, indicating strong cytotoxicity even at low concentrations.

**Conclusion:** This study establishes a rapid, cost-effective, and nontoxic protocol for the green biosynthesis of AgNPs using *H. persicum* fruit extract. The findings demonstrate that this culturally significant plant can serve as a novel, sustainable precursor for high-performance nanoparticles, offering promising potential for targeted nanomedicine and cancer therapeutics.

**Keywords:** *Cytotoxic; Green synthesis; MTT; Silver Nanoparticles; Heracleum persicum*

Copyright © 2026, This is an original open-access article distributed under the terms of the Creative Commons Attribution-noncommercial 4.0 International License which permits copy and redistribution of the material just in noncommercial usages with proper citation.

## 1. Introduction

Despite substantial advancements in cancer prevention, diagnostic strategies, and therapeutic interventions, the global burden of cancer remains a critical public health challenge affecting millions of individuals worldwide. Chemotherapy remains a cornerstone of oncological treatment; however, it fails in nearly 90% of cases involving conventional chemotherapeutics. This failure is predominantly driven by the development of multi-drug resistance (MDR), which frequently culminates in therapeutic failure and mortality (1). Increased mutation frequencies and the rapid genetic evolution of malignant cells are primary factors contributing to acquired resistance against standard anticancer agents (2). Consequently, there is an urgent clinical imperative to identify novel therapeutic agents capable of overcoming MDR in cancer management. Nanotechnology offers a promising paradigm, providing advanced tools to detect cancer cells *in vivo*, deliver cytotoxic payloads with high precision, and enhance therapeutic efficacy and selectivity (3). Over the past few decades, numerous studies have demonstrated the potent anti-angiogenic and anti-proliferative properties of silver nanoparticles (4). Metal nanoparticle synthesis typically relies on physical, chemical, biological, or photochemical reduction methods, each presenting distinct advantages and limitations depending on the reducing agents employed

(5). However, compared to conventional physical and chemical strategies, biological methods offer an eco-friendly, sustainable, safe, and cost-effective route for synthesizing stable nanomaterials (6), thereby driving a significant research shift toward green synthesis (7). Green nanotechnology—utilizing plant extracts and microorganisms—has gained considerable momentum, with expanding applications spanning materials science, medicine, pharmaceuticals, and biotechnology (8). Specifically, the biosynthesis of silver nanoparticles using medicinal plant extracts as dual reducing and capping agents has been widely investigated (9-11). During this reduction and stabilization process, various phytochemical constituents, such as flavonoids, terpenoids, carboxylic acids, aldehydes, and ascorbic acid, actively participate (12). Owing to their unique nanoscale physicochemical properties, potent bactericidal activity, and enhanced antitumor efficacy, AgNPs have emerged as one of the most versatile and widely utilized nanomaterials in biomedicine, consumer products, and the food industry (13). *Heracleum persicum* (Apiaceae) is a herbaceous species native to Iran, Iraq, and Turkey, with a widespread distribution across Europe (14). In Iranian traditional medicine, it is extensively utilized to treat a variety of pathologies, including oncological, gastrointestinal, rheumatological, neurological, urinary, and respiratory disorders (15). Phytochemical investigations have identified several classes of bioactive compounds within the plant, particularly in its fruits, including furanocoumarins, flavonoids, tannins, alkaloids, phenylpropanoids, aliphatic esters, terpenes, and carbonyl compounds (15). Recent pharmacological studies have validated these traditional uses; for instance, Sharififar et al. (2009) reported the immunomodulatory effects of *H. persicum* aqueous extracts in Swiss albino mice (16). Other studies have demonstrated the antibacterial efficacy of its essential oils against *Listeria monocytogenes* and *Escherichia coli* (17). Parallel to these botanical advancements, breast cancer remains a preeminent global public health crisis. As of 2020, breast cancer was responsible for approximately 10 million deaths worldwide. Epidemiological projections for 2022 further underscore this burden, with an estimated 287,850 new invasive cases, 51,400 cases of ductal carcinoma in situ (DCIS), and 43,250 cancer-related deaths reported globally (18). Given the intersection of plant-based bioactive compounds and cancer therapeutics, recent research has explored the biosynthesis of gold and silver nanoparticles (AgNPs) using various tissues of *H. persicum*. For example, Mohammadi et al. (2020) successfully utilized *H. persicum* extract as a biological reducing and stabilizing agent to immobilize AgNPs on magnetic polyallylamine, demonstrating significant catalytic performance in dye reduction (19). Gharari et al. synthesized silver nanoparticles using fruit extract of *H. persicum* and evaluated their antibacterial, antioxidant, and anti-proliferative activities against MDA-MB231 breast cancer cells, reporting a suppressive effect on cell growth with an $IC_{50}$ value of 82.73 µg/mL at 48 h. Similarly, Hanachi et al. (2022) investigated AgNPs biosynthesized from the stem extract of *H. persicum* and confirmed their inhibitory activity against MDA-MB231 cells, with an $IC_{50}$ value of 63.29 µg/mL at 48 h (10). Despite these advancements, the anti-proliferative activity of AgNPs biosynthesized specifically from *H. persicum* fruit extract has not yet been evaluated against the MCF-7 breast cancer cell line. To address this knowledge gap, the present study was designed to investigate the anti-proliferative potential of AgNPs synthesized via *H. persicum* fruit extract against MCF-7 cells. To the best of our knowledge, this work constitutes the first report on the biosynthesis of AgNPs using aqueous fruit extract of *H. persicum* and their subsequent cytotoxic evaluation in the MCF-7 model. These findings provide preliminary evidence of anti-proliferative potential and establish *H. persicum* fruit extract as a novel, sustainable platform for green nanotechnology in cancer therapeutics.

## 2. Materials and Methods

### 2.1 Plant Material

The fruits of *Heracleum persicum* (Apiaceae) were procured from a local commercial market in Zanjan, Iran. For taxonomic authentication, the plant material was identified and verified by Dr. Yazdinezhad at the Zanjan University of Medical Sciences.

### 2.2 Preparation of Aqueous Plant Extract

To prepare the aqueous extract, 20 g of dried, pulverized *H. persicum* powder was suspended in 350 mL of double-distilled water ($ddH_2O$). The suspension was subjected to continuous stirring using a mechanical shaker at 200 rpm for 30 min at ambient temperature (25 °C). Following incubation, the mixture was centrifuged at 5,500 rpm for 20 min. The resulting supernatant was collected and further purified via filtration through Whatman No. 1 filter paper. The prepared extract was then stored at -20 °C until further use.

### 2.3 Biosynthesis of AgNPs

The optimal parameters for AgNP synthesis were evaluated by varying the volume of *H. persicum* fruit extract (0.8, 1.6, 8, and 16 mL) added to a constant volume of 3 mM $AgNO_3$ solution (8 mL), resulting in volume ratios of 1:10, 1:5, 1:1, and 1:0.5, respectively. The resulting suspensions were stirred at 150 rpm for 1 min and subsequently incubated in the dark for 24, 48, and 72 h to mitigate the photo-reduction of Ag (I) ions. A transition to a dark brown color was observed after 72 h of incubation, signaling the successful reduction and formation of AgNPs. The optimal synthesis was achieved using a 1:1 volume ratio of fruit extract to $AgNO_3$, and with the extract serving as both the reducing and capping agent.

The biosynthesized AgNPs were isolated by centrifugation at 6,000 rpm for 15 min. The resulting pellets were washed three times with $ddH_2O$ to ensure the removal of unreacted precursors and impurities. The optical properties of the AgNPs were characterized using a UV-Vis spectrophotometer (Shimadzu UV-VIS 2550, Japan) within the wavelength range of 380–780 nm (resolution: 1 nm). The formation of AgNPs was confirmed by the presence of a characteristic Surface Plasmon Resonance (SPR) peak, observed near 450 nm.

### 2.4 Characterization of green-synthesized AgNPs

The physicochemical properties of the AgNPs biosynthesized via the aqueous fruit extract of *H. persicum* were characterized using X-ray powder diffraction (XRD), transmission electron microscopy (TEM), dynamic light scattering (DLS), and zeta potential measurements. The crystalline nature of the AgNPs was determined via XRD using a Bruker AXS-D8 Advance Cu-Kα diffractometer (Bruker, MA, USA) operating at 40 kV and 45 mA with a scanning rate of 1°/min. Dried nanoparticle samples were uniformly coated onto a sample holder, and diffraction patterns were recorded over a range of 10 °C-80 °C at 2θ angles. The morphological and structural properties of the AgNPs were examined using a Zeiss EM 900 transmission electron microscope at an accelerating voltage of 80 kV. Furthermore, the hydrodynamic particle size distribution (PSD) and colloidal stability were evaluated by measuring the zeta potential and particle size using a Zetasizer Nano ZS ZEN3600 instrument (Malvern Instruments, Malvern, UK) in an aqueous suspension **(9)**.

### 2.5 Anti-proliferative Activity of AgNPs

The anticancer potential of the synthesized AgNPs was evaluated against human MCF-7 breast cancer cells and human normal foreskin fibroblast cells (HFF-2) using the MTT [3-(4,5-dimethylthiazol-2-yl)-2,5-diphenyltetrazolium bromide] assay. Both cell lines were obtained from the Pasteur Institute (Tehran, Iran). Cells were cultured at 37 °C within a humidified 5% $O_2/CO_2$ atmosphere. The AgNPs solution was serially diluted to obtain the concentration range of 1.25–160 µg/mL. HFF-2 and MCF-7 cells were cultured in RPMI-1640 and DMEM supplemented with 10% (v/v) FBS and 100Uml$^{-1}$ penicillin/streptomycin antibiotics, respectively. For the MTT test, cells ($1\times10^5$cells/ well) were seeded onto flat-bottomed 96-well culture plates and cultured overnight, and treated with AgNPs solutions. Next, the plates were incubated for 24 and 48 h at 37°C **(20)**.

After the incubation period, the cells were incubated with 20 µL MTT solution (5 mg/mL) for 4 hours. Replacement of MTT with 100 µL DMSO resulted in the solubilization of formazan. Cell viability was measured at 570 nm using an ELISA reader after 15 min of shaking at room temperature. The plates without AgNPs were considered blanks.

The 50% inhibitory concentration ($IC_{50}$) value is determined using the following formula:

$$Viability(\%) = \frac{A\ sample}{A\ control} * 100 \quad (1)$$

### 2.6 Statistical Analysis

All experiments were performed in triplicate, and the results are presented as the mean ±\pm± standard deviation (SD). Statistical significance was determined using one-way analysis of variance (ANOVA) followed by Duncan's multiple range test. A p-value of <0.01 was considered statistically significant.

## 3. Result

### 3.1 Visual Observation and UV-vis Absorbance Spectra

The biosynthesis of AgNPs was optimized by evaluating the synergistic effects of the *H. persicum* fruit extract concentration and the incubation period, both of which are critical parameters in the biogenic reduction process. To determine the optimal extract-to-precursor ratio, varying volumes of the fruit extract (0.8, 1.6, 8, and 16 mL) were added to a fixed volume (8 mL) of 3 mM aqueous silver nitrate ($AgNO_3$) solution. The reduction of silver nitrate ions to $Ag^+$ was confirmed by the color change of the solution from colorless to yellowish brown and finally to colloidal brown (Figure 1).

The formation of AgNPs and their characteristic surface plasmon resonance (SPR) were further validated via UV-Vis spectroscopy, with absorption bands observed between 450 and 480 nm. UV-Visible spectra illustrated that the Plasmon resonance band for the 1:10, 1:5, 1:1, and 1:0.5 ratios of plant extract to $AgNO_3$ was at 457, 444, 448, and 448 nm, respectively (Figure 2).

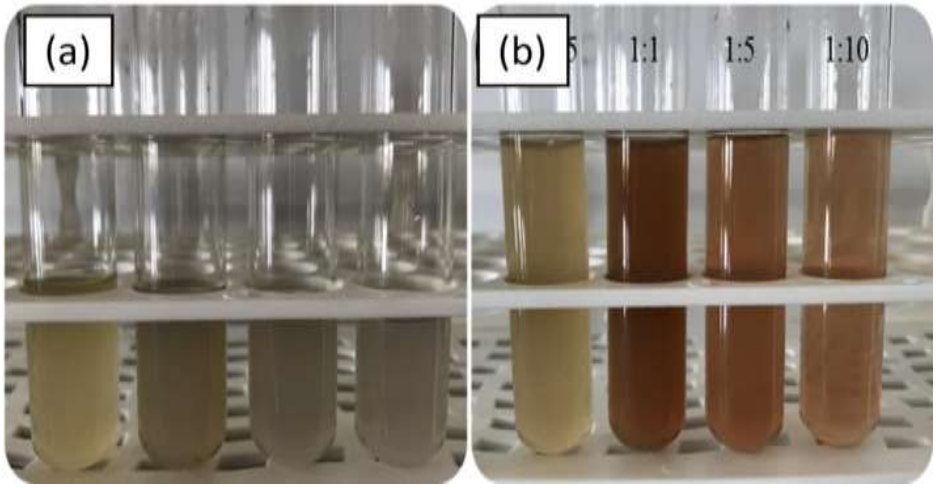



**Figure 1.** Digital optical images of AgNPs with different proportions of *H. persicum* fruit extract: silver solution (1:0.5, 1:1, 1:5, and 1:10) at different incubation periods (a) after 24 h, (b) after 72 h. **(Prepared by Authors, 2026)**.

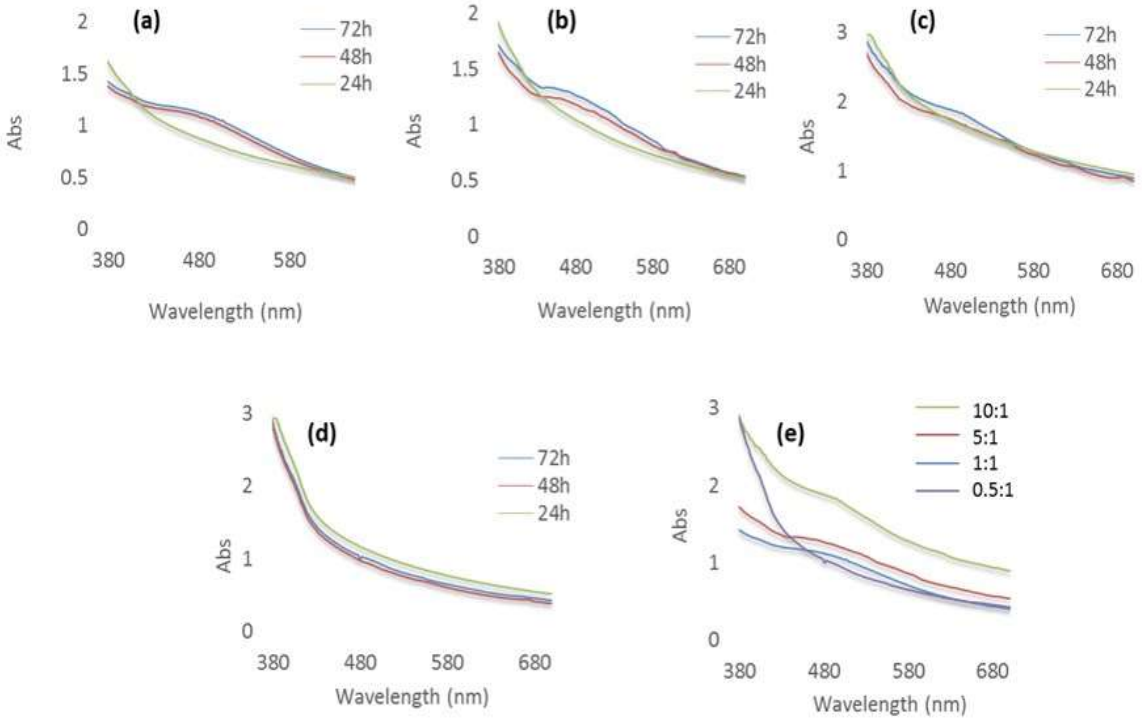



**Figure 2**. UV–vis absorption spectra of synthesized silver nanoparticles: (a) 1: 10 ratios of fruit extract: AgNO3, (b) 1: 5 ratios of fruit extract: AgNO3, (c), 1: 1 ratio of fruit extract: AgNO3 and (d) 1: 0.5 ratio of fruit extract: AgNO3, (e) different ratios of plant extract: AgNO3 at 72h. (**Prepared by Authors, 2026**).

### 3.2 TEM Analysis of AgNPs

Transmission electron microscopy (TEM) was employed to analyze the morphology and size distribution of the AgNPs. The resulting micrographs revealed that the nanoparticles were predominantly spherical in shape and exhibited a monodisperse pattern with a narrow particle size distribution (PSD). The nanoparticle diameters ranged from 5 to 45 nm, with a calculated average size of 20 nm (Figure 3).

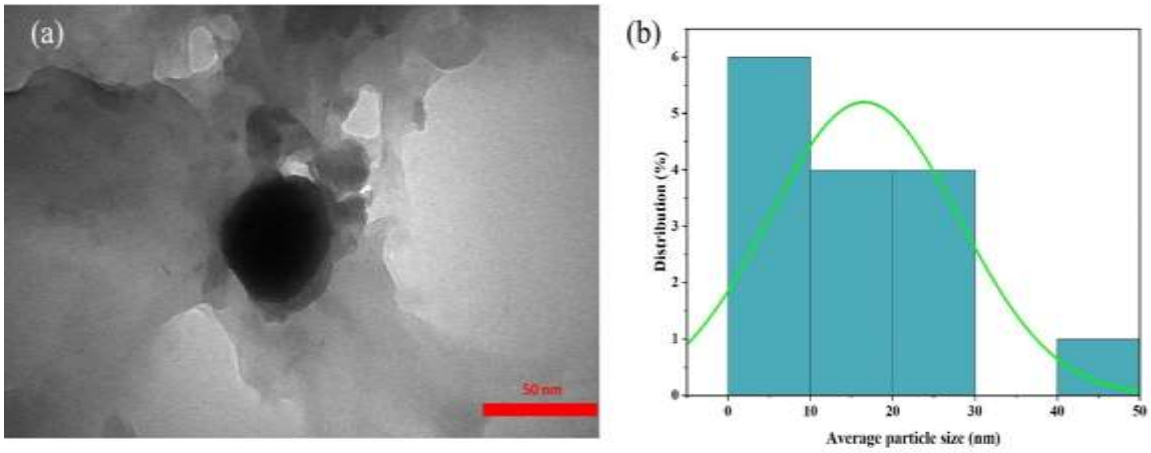



**Figure 3.** TEM micrograph (a) and histogram of PSD (b) of AgNPs synthesized from *H. persicum* fruit extract. (**Prepared by Authors, 2026**).

### 3.3 *Zeta* Potential Analysis of AgNPs

In this study, the stability of the silver nanoparticles was analyzed by zeta potential measurement. The zeta potential value of the silver nanoparticles was −8.11 mV, with a single peak, indicating their weak colloidal stability under the tested conditions, wrapped with anionic plant bio-molecules (Figure 4).

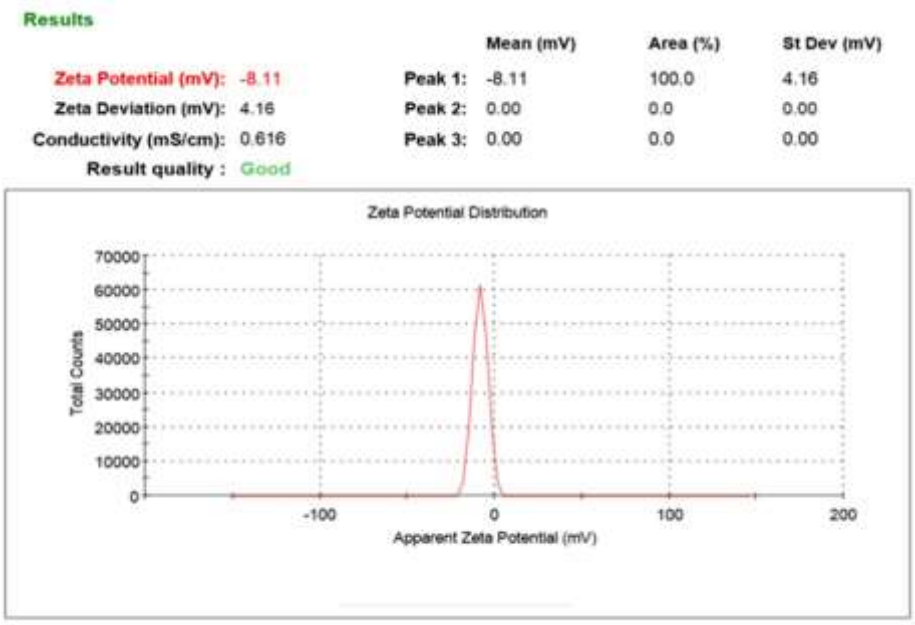



**Figure 4.** *Zeta* potential distribution of AgNPs shows negative results in mV. (**Prepared by Authors, 2026**).

### 3.4 XRD analysis of AgNPs

The crystalline nature of the biosynthesized AgNPs was confirmed via X-ray diffraction (XRD) analysis. The diffraction pattern exhibited characteristic Bragg reflection peaks corresponding to the face-centered cubic (fcc) structure of metallic silver, consistent with the Joint Committee on Powder Diffraction Standards (JCPDS) database (now maintained by the International Centre for Diffraction Data [ICDD]). The observed peaks at 2θ values of 29.5°, 33.3°, 38.2°, 44.3°, 55.1°, 57.4°, 64.8°, and 78° (Figure 5). These peaks correspond to the crystallographic planes (210), (122), (111), (200), (142), (241), (220), and (311), respectively, confirming the crystalline nature of the biosynthesized AgNPs.

The average crystallite size was estimated using the Debye–Scherrer equation, $D = K\lambda / (\beta \cos \theta)$, where D denotes the crystallite size, K is the shape factor (0.9), λ is the X-ray wavelength (0.1540598 nm), β represents the full width at half maximum (FWHM; 0.007515 rad), and θ is the Bragg angle. Based on the broadening of the (122) diffraction peak and a Bragg angle of approximately 16.65°, the calculated crystallite size was determined to be approximately 20.12 nm.

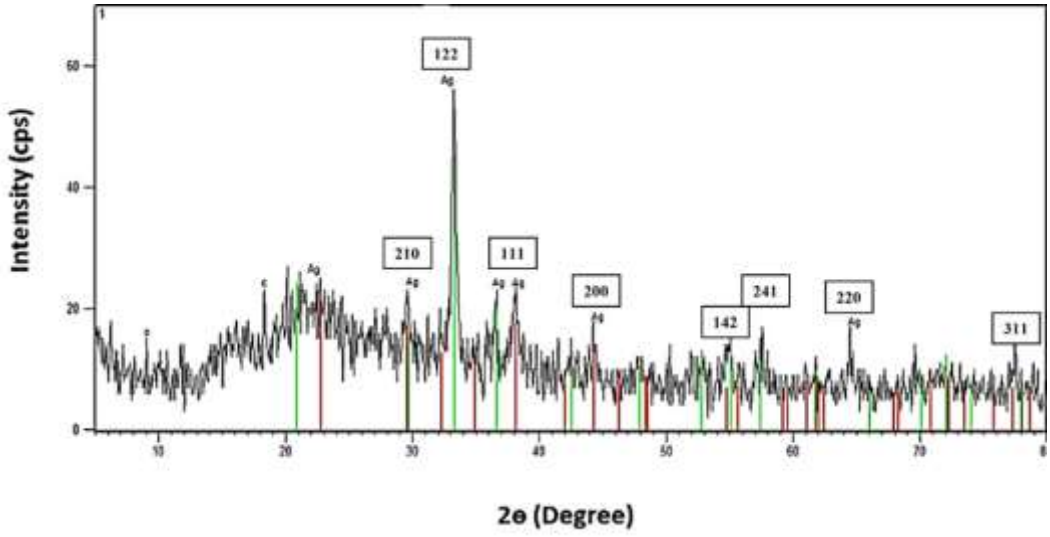



**Figure 5.** The XRD spectrum of greenly synthesized AgNPs using *H. persicum* fruit extract. (**Prepared by Authors, 2026**).

### 3.5 DLS analysis of AgNPs

Dynamic light scattering (DLS) analysis was employed to characterize the particle size distribution (PSD) of the AgNPs in aqueous suspension. The analysis revealed a mean hydrodynamic diameter of 176.8 nm, with a size range spanning from 60 to 600 nm (Figure 6).

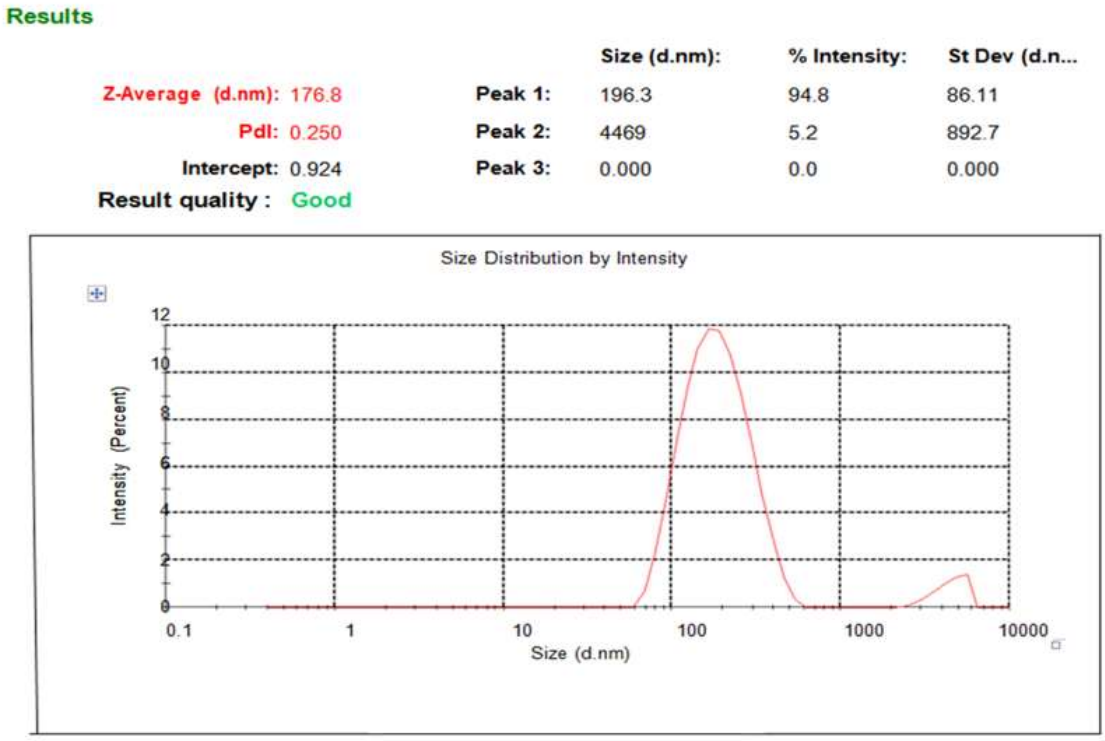



**Figure 6.** Size distribution analysis of AgNPs. (**Prepared by Authors, 2026**).

### 3.6 Anti-proliferative assessment of AgNPs on MCF-7 and HFF-2 cells

The antiproliferative efficacy of the biosynthesized AgNPs was evaluated *in vitro* using an MTT colorimetric assay against MCF-7 human breast cancer cells and HFF-2 normal human fibroblast cells. Following exposure to a concentration gradient of AgNPs (1.25–160 µg/mL) over 24 and 48 h. The results demonstrate a significant, dose- and time-dependent reduction in MCF-7 cell survival, indicating pronounced cytotoxic effects exerted by the biosynthesized nanoparticles (Figure 7)

Dose-response profiles were established via the MTT assay to quantify the antiproliferative impact of AgNPs. Comparison of the curves obtained from the 24 and 48 h assays revealed that the maximum cytotoxicity against MCF-7 and HFF-2 cells is approximately 88.44% and 84.9 % each, at 80 and 160 µg/ml AgNPs at 48 h. AgNPs treatment resulted in more significant growth inhibition in MCF-7 and HFF-2 cells with $IC_{50}$ (half maximal inhibitory concentration) values of 10.42 and 95.23 µg/ml at 24 h and 8.92 and 68.18 µg/ml at 48 h, respectively (Figure 7).

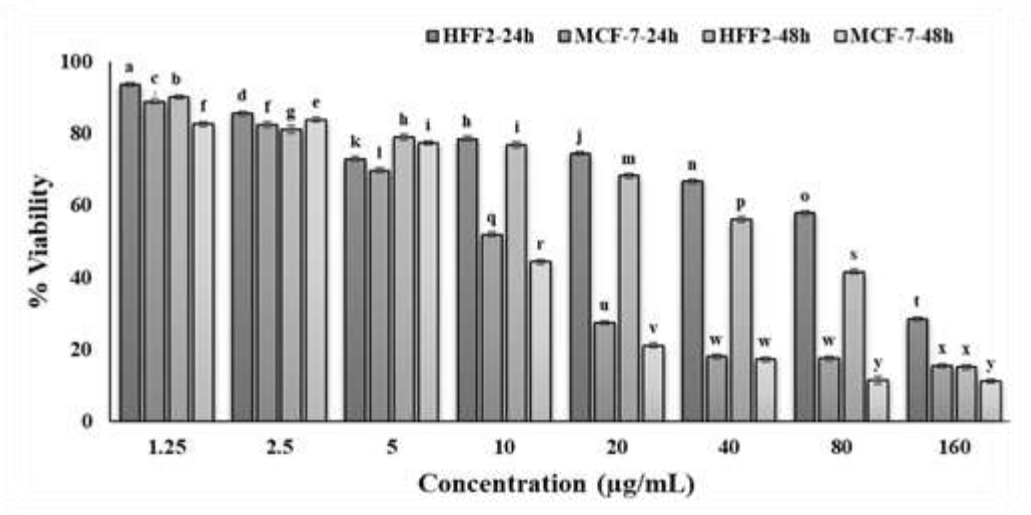



**Figure 7.** Anticancer activity of silver nanoparticles on MCF-7 and HFF-2 cells growth. The different letters denote a statistically significant difference at $P \leq 0.01$, as determined by Duncan's multiple range test. (**Prepared by Authors, 2026**).

## 4. Discussion

### 4.1 UV–Vis absorption analysis

In the present study, the aqueous fruit extract of *H. persicum* was utilized for the green biosynthesis of AgNPs. The successful reduction of silver nitrate ions to $Ag^+$ ions nanoparticles was qualitatively confirmed by the characteristic color transition of the solution from colorless to a deep brown (12). UV-Vis spectroscopy revealed the formation of AgNPs with different ratios of *H. persicum* fruit extract: silver solution at different incubation periods. It revealed plasmonic resonance of AgNPs. Plasmon resonance occurred between 450 and 480 nm, similar to those reported in the literature (21). Similarly, Ashraf et al. (2016) reported that the Plasmon resonance band for biosynthesized silver nanoparticles using *Aloe Vera* leaf extract was observed at 455 nm (22).

### 4.2 Characterization of AgNPs

#### 4.2.1 TEM analysis of AgNPs

TEM is an advanced analytical technique used for the morphological and structural identification of nanoparticles. TEM analysis confirmed that the synthesized silver nanoparticles are mostly round in shape, exhibit a monodisperse pattern, and have a narrow particle size distribution. These findings are in line with those reported by Hanachi et al. (2022) and Gharari et al. (2025), who observed that silver nanoparticles synthesized from *H. persicum* stem and fruit extracts were predominantly round and monodisperse, with average diameters of 10 nm and 35 nm, respectively (10, 23).

#### 4.2.2 Zeta Potential Intensity of AgNPs

Zeta potential is a critical parameter indicating the colloidal stability of silver nanoparticles in aqueous dispersion and thus influences their cellular uptake and cytotoxicity. In this study, the colloidal behavior of AgNPs was analyzed by zeta potential measurement. The nanoparticles exhibited a zeta potential value of −8.11 mV with a single peak, suggesting that their surface is coated with anionic phytochemicals from *H. persicum* fruit extract. Although the negative charge indicates some degree of electrostatic stabilization, the magnitude of the zeta potential falls below the commonly accepted threshold of ±30 mV for strong colloidal stability. Therefore, the AgNPs can be considered weakly stable under the tested conditions, their dispersion being primarily maintained by biomacromolecular capping rather than robust electrostatic repulsion. This implies that while the nanoparticles remain dispersed in the short term, further optimization or additional stabilizing agents may be required to enhance long-term colloidal stability (24).

#### 4.2.3 XRD Measurement of AgNPs

X-ray diffraction (XRD) is a strong, widely applied technique for assessing the crystalline structure and phase purity of nanomaterials. In this study, the XRD pattern of biosynthesized AgNPs displayed distinct diffraction peaks that confirm their crystalline metallic silver nature. Prominent reflections were observed at 2θ values of 33.3°, 38.2°, 44.3°, and 64.8°, which correspond to the (122), (111), (200), and (220) planes of the face-centered cubic (fcc) silver lattice. The observed peaks show excellent agreement with standard reference data for Ag nanoparticles (JCPDS 04-0783), validating the formation of crystalline silver nanocrystals (25). Notably, unlike many reports where the (111) reflection is dominant, this work reports the highest intensity for the (122) plane at 33.3° (26). This suggests a preferential growth orientation along the (122) plane, potentially influenced by the phytochemical constituents of *H. persicum* fruit extract acting as reducing and stabilizing agents (27). Biosynthetic routes often exhibit variations in dominant crystallographic planes due to the nature of capping biomolecules, which can alter nucleation and growth kinetics and yield distinctive crystalline orientations (27). Therefore, the prominence of the (122) plane may reflect a unique structural feature imparted by the biological synthesis pathway. The average crystallite size was calculated from the Debye–Scherrer equation using the broadening of the (122) peak, yielding approximately 20.12 nm. This value is consistent with the particle size range obtained by TEM analysis (Figure 3). The agreement between XRD and TEM results reinforces the reliability of the synthesis approach and confirms the nanoscale dimensions of the AgNPs. These findings align with previous reports on plant-mediated synthesis of AgNPs and highlight the distinctive structural characteristics imparted by *H. persicum* fruit extract (28).

#### 4.2.4 DLS Analyses of AgNPs

Dynamic Light Scattering (DLS) is an analytical technique primarily employed to estimate the hydrodynamic diameter of nanostructures in aqueous suspension. In the present study, DLS analysis of the synthesized AgNPs yielded an average size of 170 nm, with a Z-average value of 176.8 nm (Figure 6). These dimensions were notably larger than those obtained via TEM and XRD (Figure 3 and Figure 5), a discrepancy frequently observed in nanoparticle characterization. This divergence stems from the fundamental physical principles underlying each technique. While TEM and XRD probe the inorganic core, DLS measures the hydrodynamic diameter, which encompasses the metallic core along with the surrounding solvation shell and adsorbed capping agents (29). In the context of green synthesis, plant-derived metabolites—such as flavonoids, polyphenols, and proteins—adsorb onto the nanoparticle surface to form a biomolecular corona, thereby increasing the effective diameter detected by DLS (30). Furthermore, DLS is highly sensitive to nanoparticle aggregation in colloidal suspension; even minor agglomeration can significantly elevate the Z-average, as larger clusters scatter light more intensely than individual particles (31). In contrast, TEM provides direct visualization of the dried or immobilized nanoparticles, enabling accurate measurement of the electron-dense core without the influence of organic coatings or hydration layers (32). Similarly, XRD-derived sizes, calculated via the Scherrer equation, reflect only the coherent crystalline domains within the nanoparticles (26). This may be smaller than the overall particle size if the structures are polycrystalline or possess amorphous regions. Finally, DLS provides an intensity-weighted distribution that disproportionately emphasizes larger particles due to their higher scattering

intensity, potentially skewing the average size upward in polydisperse samples (33). Collectively, these methodological distinctions explain the larger DLS-derived size relative to TEM and XRD, a phenomenon particularly pronounced in green-synthesized nanoparticles due to extensive surface functionalization and colloidal behavior.

With respect to nanoparticle size reported in the literature, several studies using biological sources have demonstrated smaller dimensions. For example, Charghadchi et al. (2021) reported that AgNPs biosynthesized using *Rhus coriaria* fruit extract exhibited sizes ranging from 10 to 25 nm, with an average of 20 nm by TEM analysis (11). Gharari et al. (2022) found that Sm-AgNPs reduced with stem extract of *Scutellaria multicaulis* had an average size of approximately 60 nm (12). Similarly, Hanachi et al. (2022) reported that Hp-AgNPs synthesized from aqueous stem extract of *H. persicum* possessed a size range between 15 and 110 nm, with an average of 42 nm (10). These comparisons highlight the variability in nanoparticle dimensions depending on the biological source and synthesis conditions, and underscore the distinctive size profile of AgNPs obtained in the present study.

### 4.3 Cytotoxicity Assay of AgNPs-Treated MCF-7 Cancerous and Normal HFF-2 Cells

A growing body of literature has established the efficacy of green-synthesized AgNPs in inhibiting breast cancer cell proliferation. For instance, AgNPs fabricated using *Rhus coriaria* fruit extract have demonstrated pronounced anticancer properties against MCF-7 cells by inducing significant biochemical dysfunctions (11). Similarly, AgNPs derived from aqueous leaf-callus extracts of *Cichorium intybus* (Ci-AgNPs) and stem extracts of *Scutellaria multicaulis* (Sm-AgNPs) have shown significant cytotoxicity against MDA-MB231 cells through the enhancement of apoptotic pathways (9). Rajivgandhi et al. (2022) further confirmed the cytotoxic potential of AgNPs synthesized from *Rhizophora mucronata* leaf extract, which suppressed MCF-7 cell proliferation via apoptosis induction (34). In addition, Madakka et al. (2021) demonstrated that AgNPs derived from young leaves of *Syzygium jambolanum* exerted substantial anticancer potential on malignant MCF-7 cells (35). Collectively, these findings underscore the broad-spectrum anticancer potential of plant-mediated AgNPs across various breast cancer models, providing a robust scientific framework for the current investigation involving *H. persicum* fruit extract."

In the present study, dose–response curves were generated via MTT assay following the treatment of malignant MCF-7 cells and normal HFF-2 fibroblasts with AgNPs at concentrations ranging from 1.25 to 160 µg/mL for 24 and 48 h. The green-synthesized AgNPs exhibited a pronounced inhibitory effect on MCF-7 cell proliferation, while exerting comparatively diminished cytotoxicity toward normal HFF-2 cells. In a related study, Hanachi et al. (2022) reported that AgNPs synthesized using *H. persicum* stem extract (Hp-AgNPs) displayed significant antitumor activity against the highly aggressive MDA-MB231 cell line, achieving over 98% growth inhibition at 250 µg/mL and an $IC_{50}$ value of 63.29 µg/mL at 48 h (10). In contrast, our findings demonstrated that the AgNPs induced growth inhibition in MCF-7 cells with a markedly lower $IC_{50}$ value of 8.92 µg/mL at 48 h. Although these two studies utilized different breast cancer cell lines with distinct biological characteristics and resistance profiles, this comparison highlights the potent cytotoxic potential of fruit-derived AgNPs, even against the relatively less resistant MCF-7 line, thereby underscoring their promise for targeted green nanomedicine applications.

It is important to note, however, that in the present study, the cytotoxicity of AgNPs against MCF-7 cells was evaluated solely via the MTT assay. While the MTT assay is a standard method for assessing cell viability and proliferation, it provides preliminary evidence rather than a comprehensive characterization of the underlying anti-proliferative mechanisms. Consequently, further investigations, including apoptosis detection, ROS generation assays, and *in vivo* studies, are required to confirm and further elucidate the anti-proliferative potential of these AgNPs.

## 5. Conclusion

The present study demonstrated the successful application of *H. persicum* fruit extract for the rapid, stable, and eco-friendly biosynthesis of biologically active AgNPs. Unlike previous reports that relied on chemical reducing agents or other plant sources, our method uniquely harnesses the phytochemical richness of *H. persicum* fruit as natural reducing and stabilizing agents. This not only eliminates the need for toxic chemicals but also provides enhanced stability and biocompatibility to the nanoparticles. The biosynthesized AgNPs showed strong cytotoxicity against MCF-7 cells, with low $IC_{50}$ values at both 24 and 48 h, confirming their strong anti-proliferative potential even at minimal concentrations. The novelty of this work lies in introducing *H. persicum* as a new green synthesis platform, thereby expanding the repertoire of medicinal plants employed in nanotechnology. These findings suggest that AgNPs could serve as promising candidates for nanomedicine applications, particularly in breast cancer therapy, while also offering an environmentally sustainable manufacturing route. Future studies should focus on *in vivo* validation and mechanistic insights to further translate these nanoparticles into industrial and clinical applications.

## 6. Declarations

### 6.1 Acknowledgments

This work has been supported by Zanjan University of Medical Sciences, Zanjan, Iran, under a Pharm. D. thesis proposal (Code No. A-12-307-33).

### 6.2 Ethical Considerations

All accepted principles of ethical and professional conduct have been followed. (Ethical Code: IR-ZUMS. REC. 1398.299)

## 6.3 Authors' Contributions

B. R., A. S. and Z.G. performed the experiments. Z. G. and A.S. wrote the main manuscript text. A. Y., A.S. and S. S. supervised the project. All authors reviewed the manuscript.

## 6.4 Conflict of Interest

The authors declare no conflicts of interest.


## 6.5 Fund or Financial Support

The authors received no financial support or funding for this study.


## 6.6 Using Artificial Intelligence Tools (AI Tools)

The authors utilized Grammarly solely for language polishing, proofreading, and minor grammatical corrections. No generative AI tools were employed for data analysis, content generation, or scientific writing.

## References


1. Alfarouk KO, Stock C-M, Taylor S, Walsh M, Muddathir AK, Verduzco D, et al. Resistance to cancer chemotherapy: failure in drug response from ADME to P-gp. Cancer Cell Int. 2015;15(1):1-13. [DOI:10.1186/s12935-015-0221-1] [PMID] [PMCID]

2. Kreso A, O'Brien CA, Van Galen P, Gan OI, Notta F, Brown AM, et al. Variable clonal repopulation dynamics influence chemotherapy response in colorectal cancer. Sci. 2013;339(6119):543-8. [DOI:10.1126/science.1227670] [PMID] [PMCID]

3. Jin C, Wang K, Oppong-Gyebi A, Hu J. Application of nanotechnology in cancer diagnosis and therapy-a mini-review. Int J Med Sci. 2020;17(18):2964. [DOI:10.7150/ijms.49801] [PMID] [PMCID]

4. Simon S, Sibuyi NRS, Fadaka AO, Meyer S, Josephs J, Onani MO, et al. Biomedical applications of plant extract-synthesized silver nanoparticles. Biomedicines. 2022;10(11):2792. [DOI:10.3390/biomedicines10112792] [PMID] [PMCID]

5. Parveen K, Banse V, Ledwani L, editors. Green synthesis of nanoparticles: their advantages and disadvantages. AIP conference proceedings; 2016: AIP Publishing LLC. [DOI:10.1063/1.4945168]

6. Guan Z, Ying S, Ofoegbu PC, Clubb P, Rico C, He F, et al. Green synthesis of nanoparticles: Current developments and limitations. Environ Technol Innov. 2022:102336. [DOI:10.1016/j.eti.2022.102336]

7. Jeyaraj M, Rajesh M, Arun R, MubarakAli D, Sathishkumar G, Sivanandhan G, et al. An investigation on the cytotoxicity and caspase-mediated apoptotic effect of biologically synthesized silver nanoparticles using Podophyllum hexandrum on human cervical carcinoma cells. Colloids Surf B Biointerfaces. 2013;102:708-17. [DOI:10.1016/j.colsurfb.2012.09.042] [PMID]

8. Pokrajac L, Abbas A, Chrzanowski W, Dias GM, Eggleton BJ, Maguire S, et al. Nanotechnology for a sustainable future: Addressing global challenges with the international network4sustainable nanotechnology. ACS Publications; 2021. [DOI:10.1021/acsnano.1c10919] [PMID]

9. Gharari Z, Hanachi P, Sadeghinia H, Walker TR. Cichorium intybus bio-callus synthesized silver nanoparticles: A promising antioxidant, antibacterial and anticancer compound. Int J Pharm. 2022;625:122062.

[DOI:10.1016/j.ijpharm.2022.122062] [PMID]

10. Hanachi P, Gharari Z, Sadeghinia H, Walker TR. Synthesis of bioactive silver nanoparticles with eco-friendly processes using Heracleum persicum stem extract and evaluation of their antioxidant, antibacterial, anticancer and apoptotic potential. J Mol Struct. 2022:133325. [DOI:10.1016/j.molstruc.2022.133325]

11. Charghadchi M, Gharari Z, Sadighian S, Yazdinezhad A, Sharafi A. Green synthesized silver nanostructure using Rhus coriaria fruit extract inhibits the growth of malignant MCF-7 Cell Line. Braz Arch Biol Technol. 2022;64. [DOI:10.1590/1678-4324-2021210069]

12. Gharari Z, Hanachi P, Walker TR. Green synthesized Ag-nanoparticles using Scutellaria multicaulis stem extract and their selective cytotoxicity against breast cancer. Anal Biochem. 2022;653:114786.

[DOI:10.1016/j.ab.2022.114786] [PMID]

13. Zhang XF, Liu Z-G, Shen W, Gurunathan S. Silver nanoparticles: synthesis, characterization, properties, applications, and therapeutic approaches. Int J Mol Sci. 2016;17(9):1534. [DOI:10.3390/ijms17091534] [PMID]

14. Fröberg L. Heracleum L. Flora nordica. 2010;6:224-34.

15. Majidi Z, Lamardi SS. Phytochemistry and biological activities of Heracleum persicum: A review. J Integr Med. 2018;16(4):223-35. [DOI:10.1016/j.joim.2018.05.004] [PMID]

16. Sharififar F, Pournourmohammadi S, Arabnezhad M, Rastegarianzadeh R, Ranjbaran O, Pourhemati A. Immunomodulatory activity of

aqueous extract of Heracleum persicum Desf. in mice. Iran J Pharm Res. 2010;8(4):e128651.

17. Rezayan A, Ehsani A. Evaluation of the chemical compounds and antibacterial properties of the aerial parts of Persian Heracleum persicum essence. JBUMS. 2015;17(6):26-32.

18. Giaquinto AN, Sung H, Miller KD, Kramer JL, Newman LA, Minihan A, et al. Breast cancer statistics, 2022. CA: Cancer J. Clin. 2022;72(6):524-41. [DOI:10.3322/caac.21754] [PMID]

19. Mohammadi P, Heravi MM, Sadjadi S. Green synthesis of Ag NPs on magnetic polyallylamine decorated g-C3N4 by Heracleum persicum extract: efficient catalyst for reduction of dyes. Sci. Rep. 2020;10(1):6579. [DOI:10.1038/s41598-020-63756-4] [PMID] [PMCID]

20. Gharari Z, Aghajanzadeh M, Sharafi A. Scutellaria orientalis subsp. Bornmuelleri: phytochemical composition and biological activities. Nat Prod Res. 2022;36(5):1385-90. [DOI:10.1080/14786419.2021.1875463] [PMID]

21. Satapathy SR, Mohapatra P, Preet R, Das D, Sarkar B, Choudhuri T, et al. Silver-based nanoparticles induce apoptosis in human colon cancer cells mediated through p53. Nanomed. 2013;8(8):1307-22. [DOI:10.2217/nnm.12.176] [PMID]

22. Ashraf J, Ansari M, Khan H, et al. Green synthesis of silver nanoparticles and characterization of their inhibitory effects on AGEs formation using biophysical techniques. Sci Rep. 2016; 6: 20414. [DOI:10.1038/srep20414] [PMID] [PMCID]

23. Gharari Z, Sadeghinia H, Hanachi P. Silver nanoparticles, synthesized using Heracleum persicum fruit extract: selective cytotoxicity against MDA-MB231 cells and potential antimicrobial and antioxidant activities. Nanochem Res. 2025:e230291.

24. Jadhav K, Deore S, Dhamecha D, Hr R, Jagwani S, Jalalpure S, et al. Phytosynthesis of silver nanoparticles: characterization, biocompatibility studies, and anticancer activity. ACS Biomater Sci Eng. 2018;4(3):892-9. [DOI:10.1021/acsbiomaterials.7b00707] [PMID]

25. Mehta B, Chhajlani M, Shrivastava B, editors. Green synthesis of silver nanoparticles and their characterization by XRD. J Phys Conf Ser; 2017: IOP Publishing. [DOI:10.1088/1742-6596/836/1/012050]

26. Bykkam S, Ahmadipour M, Narisngam S, Kalagadda VR, Chidurala SC. Extensive studies on X-ray diffraction of green synthesized silver nanoparticles. Adv Nanopart. 2015;4(1):1-10. [DOI:10.4236/anp.2015.41001]

27. Eker F, Akdaşçi E, Duman H, Bechelany M, Karav S. Green synthesis of silver nanoparticles using plant extracts: A comprehensive review of physicochemical properties and multifunctional applications. Int J Mol Sci. 2025;26(13):6222. [DOI:10.3390/ijms26136222] [PMID] [PMCID]

28. Ali MH, Azad MAK, Khan K, Rahman MO, Chakma U, Kumer A. Analysis of crystallographic structures and properties of silver nanoparticles synthesized using PKL extract and nanoscale characterization techniques. ACS Omega. 2023;8(31):28133-42. [DOI:10.1021/acsomega.3c01261] [PMID] [PMCID]

29. Mahto M, Priya S, Thakur S, Paramanik P, Verma R, Mahato P. A comprehensive review of green synthesis, characterization and biomedical applications of silver nanoparticle synthesized using plant extracts. World J Adv Res Rev. 2024;22(3):1950-77. [DOI:10.30574/wjarr.2024.22.3.1899]

30. Shoily MT, Hossain MM, Das SC, Bedoura S. Green synthesis of silver nanoparticles using Calathea ornata extract: Characterization, antimicrobial properties, and cytotoxicity assessment. MRS Adv. 2025:1-7. [DOI:10.1557/s43580-025-01373-x]

31. Yeap SP, Lim J, Ngang HP, Ooi BS, Ahmad AL. Role of particle-particle interaction towards effective interpretation of Z-average and particle size distributions from dynamic light scattering (DLS) analysis. J Nanosci Nanotechnol. 2018;18(10):6957-64. [DOI:10.1166/jnn.2018.15458] [PMID]

32. Modena MM, Rühle B, Burg TP, Wuttke S. Nanoparticle characterization: what to measure? Adv Mater. 2019;31(32):1901556. [DOI:10.1002/adma.201901556]

33. Farkas N, Kramar JA. Dynamic light scattering distributions by any means. J Nanopart Res. 2021;23(5):120. [DOI:10.1007/s11051-021-05220-6] [PMID] [PMCID]

34. Rajivgandhi GN, Ramachandran G, Kannan MR, Velanganni AAJ, Siddiqi MZ, Alharbi NS, et al. Photocatalytic degradation and anti-cancer activity of biologically synthesized Ag NPs for inhibit the MCF-7 breast cancer cells. J King Saud Univ Sci. 2022;34(1):101725. [DOI:10.1016/j.jksus.2021.101725]

35. Madakka M, Jayaraju N, Rajesh N. Evaluating the antimicrobial activity and antitumor screening of green synthesized silver nanoparticles compounds, using Syzygium jambolanum, towards MCF7 cell line (Breast cancer cell line). J Photochem Photobiol. 2021;6:100028. [DOI:10.1016/j.jpap.2021.100028]